Sensors and Materials, Vol. 22, No. 3 (2010) 135–142
MYU Tokyo

S & M 0795

Design and Fabrication of a Scanning Near-Field Microscopy Probe with Integrated Zinc Oxide Photoconductive Antennas for Local Terahertz Spectroscopy

Kentaro Iwami*, Takahito Ono[1] and Masayoshi Esashi[2]

Division of Advanced Mechanical Systems Engineering,
Tokyo University of Agriculture and Technology,
2-24-16 Nakacho, Koganei, Tokyo 184-8588, Japan
[1]Department of Mechanical Systems and Design, Tohoku University, Sendai, Japan
[2]WPI Advanced Institute of Materials Research, Tohoku University, Sendai, Japan

Key words: micro-electromechanical systems (MEMS), terahertz, scanning near-field optical microscopy, terahertz time-domain spectroscopy, zinc oxide

In this paper, we report the design and fabrication of a scanning near-field optical microscopy (SNOM) probe with integrated zinc oxide photoconductive antennas for local terahertz (THz) spectroscopy. Photoconductive antennas are used as a THz pulse emitter and detector. A pyramidal tip with an aperture formed at the end of a silicon cantilever is used as an SNOM head.

1. Introduction

The terahertz (THz) region of the electromagnetic spectrum has attracted interest in many research fields.[1–3] Spectroscopic measurement in this region (i.e., THz spectroscopy) is one of the most attractive applications of THz waves because of its ability to provide molecular identification by fingerprint vibrations,[2] which correspond to specific optical responses of the sample. A fingerprint vibration in the THz region identifies not only the molecular species, but also intermolecular interactions such as crystallographic polymorphism,[4] molecular cluster size,[5] and protein folding.[6] The technology that provides real-time identification and positioning of molecular species and intermolecular interactions on the surface (molecular mapping) using THz spectroscopy will be a very useful analysis tool for surface science and nanotechnology.

THz time-domain spectroscopy[7] (THz-TDS) is widely used for THz-spectroscopy because of its broad bandwidth and ability to measure a specimen's complex refractive index. A typical THz-TDS system consists of a THz pulse emitter, detector, and femtosecond pulse laser, which excites the emitter and gates the detector. THz imaging

*Corresponding author: e-mail: k_iwami@cc.tuat.ac.jp

technology combined with THz spectroscopy is an emerging technology for molecular mapping. However, the long wavelength of THz waves (30–3,000 μm) limits the spatial resolution of molecular mapping.

Scanning near-field optical microscopy (SNOM) can realize subwavelength resolutions beyond the diffraction limit. Recently, SNOM technology has been applied to THz-TDS (THz-SNOM), and has realized nanoscale spatial resolution of THz images.[8] In this system, a SNOM probe is added to the THz-TDS system. These components are often placed in a vacuum chamber to avoid moisture absorption for measuring THz waves. This vacuum environment makes in vitro measurement of living cells difficult.

To achieve near-field THz-TDS measurement in ambient atmosphere, the optical path of a THz wave must be inserted in a waveguide structure. This requires a smart THz SNOM probe with an integrated THz wave emitter and detector. In this paper, we report the design and fabrication of a novel THz-SNOM microprobe, which performs THz-TDS measurements using an integrated emitter and a detector.

2. Materials and Methods

2.1 *Device design*

Photoconductive antennas have been adopted both as the THz emitter and detector for the microprobe. The photoconductive antenna is the most suitable for integration with a SNOM probe because it is a planar device, and acts as both an emitter and a detector.[9] Gallium arsenide (GaAs) formed by molecular beam epitaxy (MBE) at a low-temperature (LT-GaAs) is often used as a photoconductive material because of its high resistivity, high breakdown voltage, and short carrier lifetime, which are attractive characteristics for THz-TDS.[10] However, the growth of the LT-GaAs is limited on GaAs substrates. Hence, integration of LT-GaAs devices with SNOM probes based on the advanced Si microfabrication technology is difficult. Therefore, an assembly process is required to fabricate the microprobe with LT-GaAs antenna.[11] Zinc oxide (ZnO) single crystals have also been reported as photoconductive materials for THz applications,[12] but they cannot be used with the microprobe because of process limitations. In contrast, the characteristics of sputter-deposited ZnO vary widely.[13] Sputtered ZnO is process compatible with Si microfabrication and exhibits superior photoconductive characteristics under appropriate sputtering conditions. However, there are few reports on THz application of photoconductive antennas using ZnO thin films. We used sputter-deposited ZnO with a resistivity of 9.6×10^4 Ω·cm as a photoconductive material for the THz emitter and detector, which exhibited ultrafast pulse emission with a bandwidth of up to about 0.4 THz.[14] In this paper, we report the integration of the ZnO photoconductive antenna with a scanning near-field optical microscopy probe using an advanced microfabrication technology.

Figure 1 shows a schematic of the microprobe. A silicon cantilever was used. The photoconductive antenna structures are made of a photoconductive thin film and metal patterns; therefore, they are highly compatible with the advanced Si microfabrication processes. A silicon dioxide pyramidal tip covered with a metal thin film is used as the

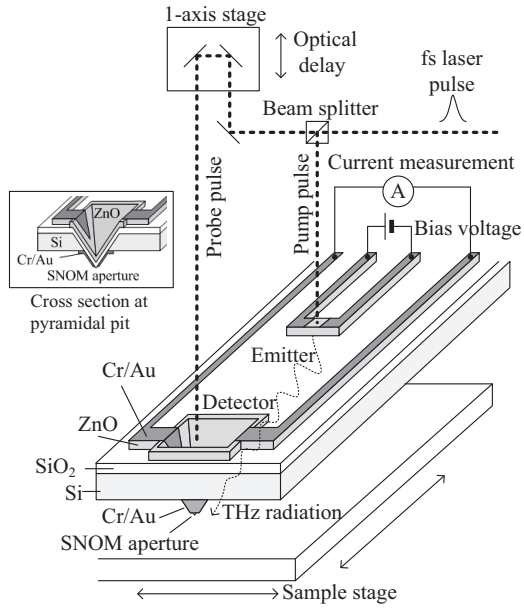

Fig. 1. Schematic of local THz spectroscopy system using a near-field microprobe with an integrated THz pulse emitter and detector.

SNOM probe. By using the microfabricated probe structure, simultaneous topographic images can be acquired by atomic force microscopy (AFM).

2.2 *Fabrication*

Figure 2 shows vertical and cross-sectional images of a THz near-field microprobe. In this structure, the distance between the SNOM aperture and detector antenna was determined from the thicknesses of the SiO_2 and photoconductive layers. The polarization of the THz pulse depends on the pattern of the antenna electrode. Hence, two types of antenna, one parallel and the other perpendicular to the long axis of the probe, were formed for the emitters and detectors to investigate the polarization dependence of a sample. Figure 3 shows the fabrication process flow of this probe. A solid pyramidal SNOM probe was fabricated from a Si wafer by bulk-micromachining technology. Details of each process are as follows. A (100)-oriented silicon wafer with a thickness of 400 μm is used as a substrate (Fig. 3(a)). High-resistive silicon (>1,000 Ω·cm) is chosen as the substrate material. A 500-nm-thick SiO_2 layer is formed by thermal oxidization. Photolithography is performed and square openings in the SiO_2 layer are formed by wet etching in a buffered hydrofluoric acid (BHF) solution at 36°C. The silicon substrate is anisotropically etched at 80°C for 2 h in a 20 vol.% water solution of tetramethylammonium hydroxide (TMAH), and a 60-μm-deep pyramidal

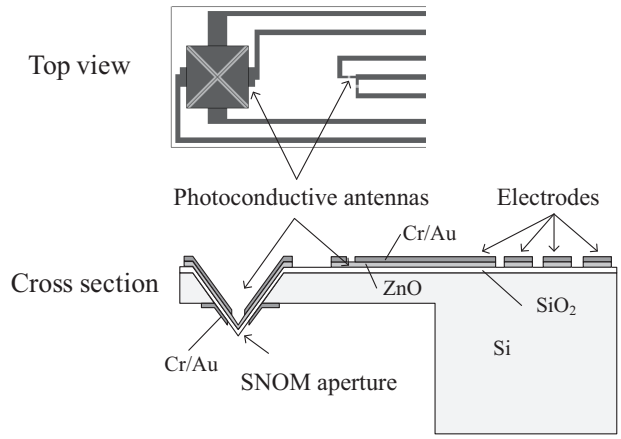

Fig. 2. Schematic of a THz near-field microprobe.

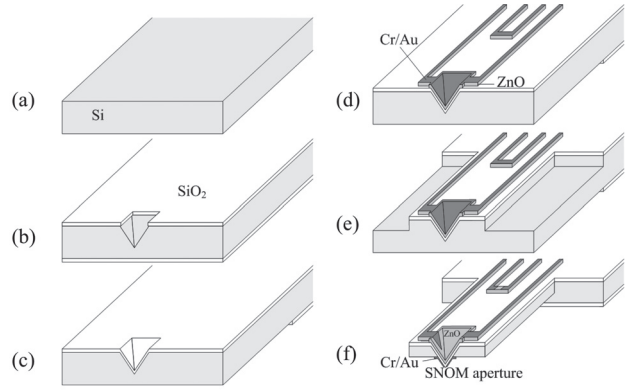

Fig. 3. Fabrication of a THz near-field microprobe.

cavity is formed (Fig. 3(b)). The SiO_2 layers are removed by BHF and the substrate is thermally oxidized again. The SiO_2 layer on the backside is patterned to form an etching mask (Fig. 3(c)). A ZnO film was formed using an rf magnetron sputter. In this process, a ZnO target with a purity of 99.99% (Furuuchi Kagaku Inc., Japan) is used. The partial pressures of argon and oxygen gas are 0.4 and 0.1 Pa, respectively. The 700-nm-thick film is deposited by sputtering with 300 W rf power for 1 h. Cr/Au layers for the antenna electrode are sputtered on the ZnO layer. Electrode patterns are formed by photolithography. The designed widths of the coplanar strip and emitter antenna were 10 and 5 μm, respectively. In this step, the Cr/Au layer on the pyramidal pit is covered by photoresist, because patterning at the pyramidal cavity is difficult owing to its depth of 60 μm. The Au layer is etched in a potassium iodine solution. Cr and ZnO layers are

etched in a cerium ammonium nitrate solution (Fig. 3(d)). The SiO_2 layer is patterned by photolithography and wet etching using BHF to make probe patterns. The probe patterns are defined by deep reactive ion etching (deep-RIE) of silicon using the typical steps of the Bosch process[15] at a depth of 40 μm (Fig. 3(e)). Probe structures are released using deep-RIE of silicon from the back side. In this step, the SiO_2 layer patterned in step (c) is used as the etching mask. The Cr/Au layers are deposited as a metal screen on the tip side of the probe by stencil mask evaporation. An antenna gap and a SNOM aperture are formed by focused ion beam (FIB) milling of the Cr/Au layers. At the pyramidal etch pit, an ion beam is scanned along the edge, and the Cr/Au electrode is divided into four parts. These electrodes are used as photoconductive detectors. A 10×10 μm^2 aperture is formed on the back side of a probe (Fig. 3(f)). Scanning electron microscopy (SEM) images of the fabricated probe are shown in Fig. 4. The four-part detector antenna pattern is successfully fabricated. However, the ZnO layer at the emitter antenna disappeared after the FIB milling. One possible reason for this disappearance is that the etching time in cerium ammonium nitrate was too long, removing ZnO underneath the mask layer by side etching. Widening the antenna or designing a 4-part triangular emitter antenna, similar to the detector antenna, may prevent the disappearance.

3. Results and Discussion

The pulse detection characteristics of the fabricated microprobe were evaluated using a THz-TDS setup, as shown in Fig. 5. In this experiment, instead of an integrated antenna, an external planar ZnO photoconductive antenna that we fabricated previously[14] was used as a pulse emitter. The typical pulse width obtained using the antenna was 50 ps and contained a 1 GHz-0.4 THz frequency component. The planar antenna was situated 3 mm away from the SNOM aperture. The THz pulse emitted from the planar antenna reaches the detector antenna through the SNOM aperture. A femtosecond (fs) laser was used as a gate for pulse emission and detection. A Ti:sapphire fs laser (CPA-2001, Clark-MXR Inc., USA) was used. The pulse width, wavelength and

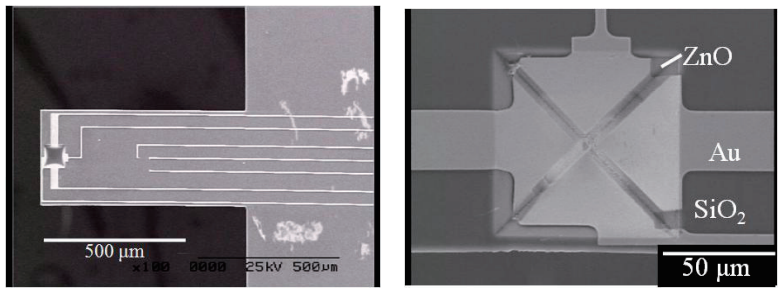

(a) (b)

Fig. 4. SEM images of fabricated THz near-field microprobe: (a) top view and (b) close-up of pyramidal etch pit.

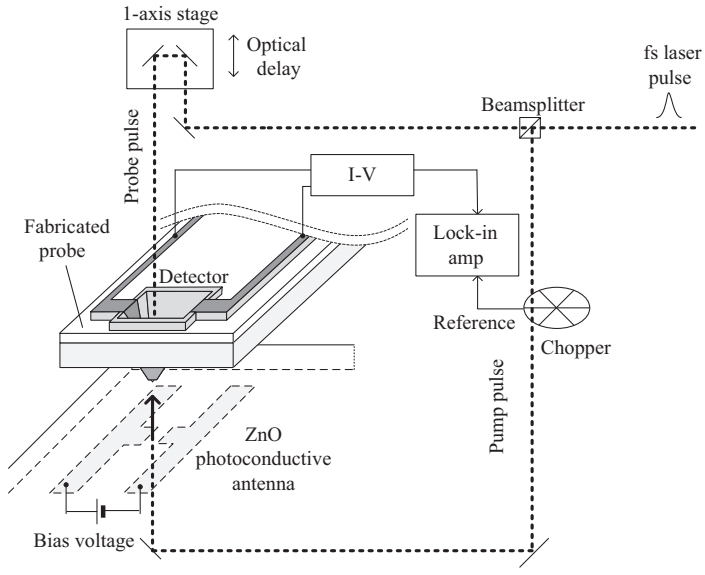

Fig. 5. Experimental setup for the demonstration of the integrated detector.

the repetition rate of the pulse are 150 fs, 775 nm and 1.2 kHz, respectively. The time delay of the fs pulse for the detector is changed by a one-axis stage. A dc bias voltage of 20 V is applied to the emitter antenna. Flowing current in the detector antenna is amplified by an I-V amplifier and a digital lock-in amplifier. The scattered light at the aperture is detected by a phototransistor, and its signal is used as a reference for the lock-in amplifier.

Figure 6 shows the detected signal in time-domain (inset) and its spectrum. Although the time-domain response is noisy, a pulse-shaped response, which is several 10 ps wide, is detected. This response is similar to that detected by a planar ZnO photoconductive detector,[14] suggesting that the integrated detector works properly. In the spectrum, as the frequency increases, the signal intensity decreases, and then the variance of intensity increases in the frequency region higher than 0.1 THz. From this result, a sub-terahertz pulse detection using the integrated antenna is demonstrated. It indicates that the probe can be used for local spectroscopic measurement. The peak voltage of the signal detected by the integrated detector with the SNOM aperture is about 200 times smaller than that detected by a planar ZnO photoconductive detector without the SNOM aperture,[14] and the signal-to-noise ratio is decreased. Because the detected signal is proportional to the electric field at the detector, the energy throughput of the aperture is calculated to be 2.5×10^{-5}. Since the size of the aperture corresponds to $\lambda/30$ at 1 THz, the order of magnitude of the throughput is reasonable when considering the magnitude of the pyramidal aperture in the visible region.[16] The signal-to-noise ratio will be improved by adopting a high-throughput aperture, such as a bow-tie shape.[17]

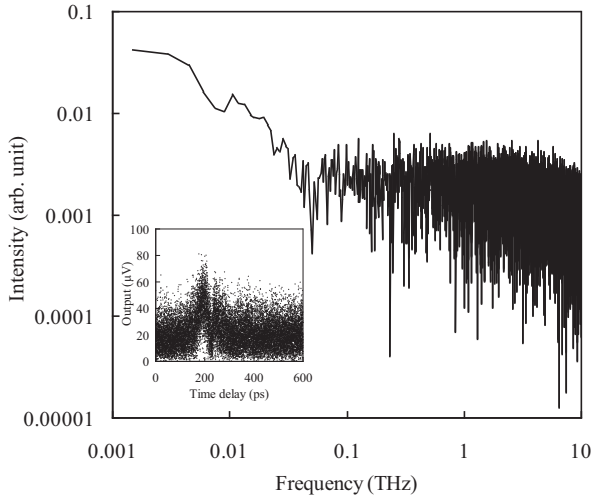

Fig. 6. Spectrum detected by integrated ZnO photoconductive antenna and its time-domain response (inset).

4. Conclusion

A THz near-field microprobe with an integrated THz emitter and detector for THz-TDS is proposed, designed, and fabricated. Photoconductive antennas made from sputter-deposited ZnO are adopted as the THz emitter and detector because of process compatibility. A pyramidal tip with an aperture formed at the end of a silicon cantilever is used as the SNOM head. Sub-THz pulse detection is demonstrated using the external photoconductive antenna and the integrated detector antenna.

Acknowledgements

Part of this work was performed at the Micro/Nanomachining Research Education Center of Tohoku University. This work was partially supported by a Grant-in-Aid for Scientific Research from the Japanese Society for the Promotion of Science (JSPS), and by Special Coordination Funds for Promoting Science and Technology, Formation of Innovation Center for Fusion of Advanced Technologies.

References

1 B. Ferguson and X.-C. Zhang: Nat. Mat. **1** (2002) 26.
2 K. Kawase, Y. Ogawa, Y. Watanabe and H. Inoue: Opt. Exp. **11** (2003) 2549.
3 D. Clery: Science **297** (2002) 763.
4 C. J. Strachan, P. F. Taday, D. A. Newnham, K. C. Gordon, J. A. Zeitler, M. Pepper and T. Rades: J. Pharmaceut. Sci. **94** (2005) 837.

5 A. M. Fedor and T. M. Korter: Chem. Phys. Lett. **429** (2006) 405.
6 A. G. Markelz, A. Roitberg and E. J. Heilweil: Chem. Phys. Lett. **320** (2000) 42.
7 M. van Exter, Ch. Fattinger and D. Grischkowsky: Opt. Lett. **14** (1989) 1128.
8 H. Lin, S. P. Mickan and D. Abbott: Proc. SPIE **6414** (2006) 64140L.
9 D. H. Auston, K. P. Cheung and P. R. Smith: Appl. Phys. Lett. **45** (1984) 284.
10 M. Tani, S. Matsuura, K. Sakai and S. Nakashima: Appl. Opt. **36** (1997) 7853.
11 K. Iwami, T. Ono and M. Esashi: Jpn. J. Appl. Phys. **48** (2008) 8095.
12 S. Ono, H. Murakami, A. Quema, G. Diwa, N. Sarukura, R. Nagasaka and Y. Ichikawa: Appl. Phys. Lett. **87** (2005) 261112.
13 J. Lee, W. Gao, Z. Li, M. Hodgson, J. Metson, H. Gong and U. Pal: Appl. Phys. A **80** (2005) 1641.
14 K. Iwami, T. Ono and M. Esashi: IEEJ Trans. Sens. Micromachines **125-E** (2007) 508.
15 C. Chang, Y.-F. Wang, Y. Kanamori, J.-J. Shih, Y. Kawai, C.-K. Lee, K.-C. Wu and M. Esashi: J. Micromech. Microeng. **15** (2005) 580.
16 P. N. Minh, T. Ono and M. Esashi: Rev. Sci. Instrum. **71** (2000) 3111.
17 K. Ishihara, K. Ohashi, T. Ikari, H. Minamide, H. Yokoyama, J. Shikata and H. Ito: Appl. Phys. Lett. **89** (2006) 201120.